Supporting Information

Synergetic degradation of organic dyes and Cr(VI) by piezocatalytic BZT-*x*BCT

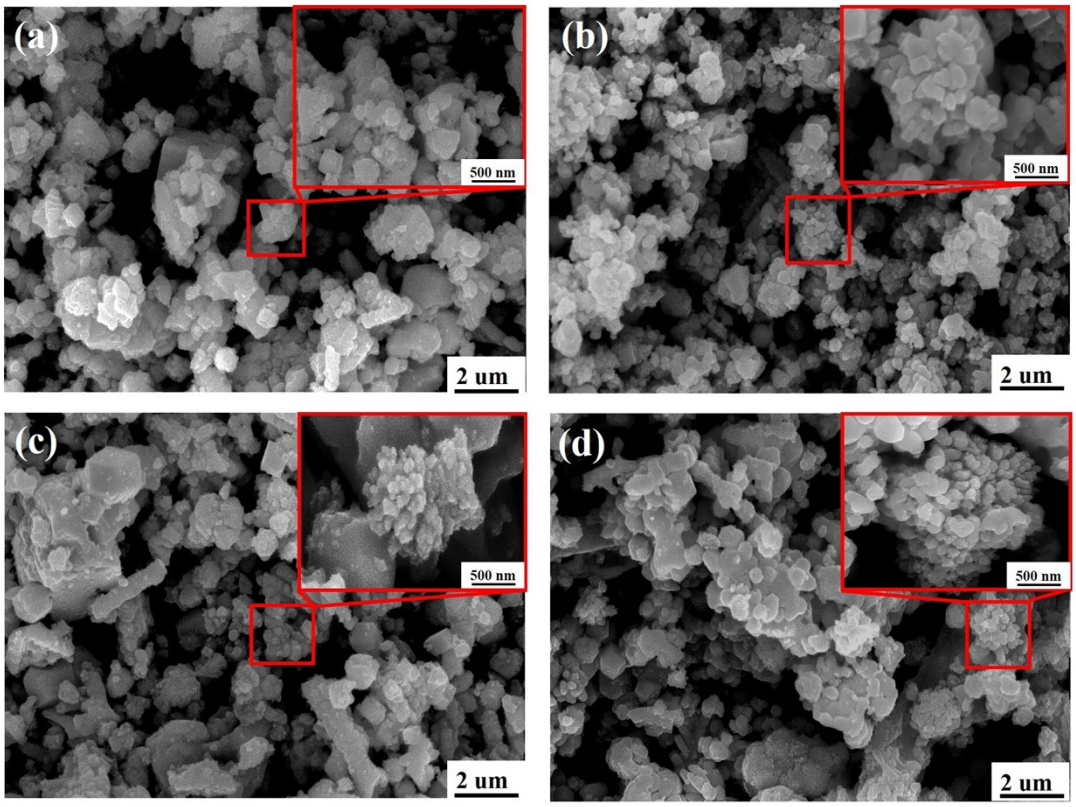

Figure S1. (a-d) FESEM image of BZT-*x*BCT samples (*x*=0.4, 0.5, 0.6, 0.7).

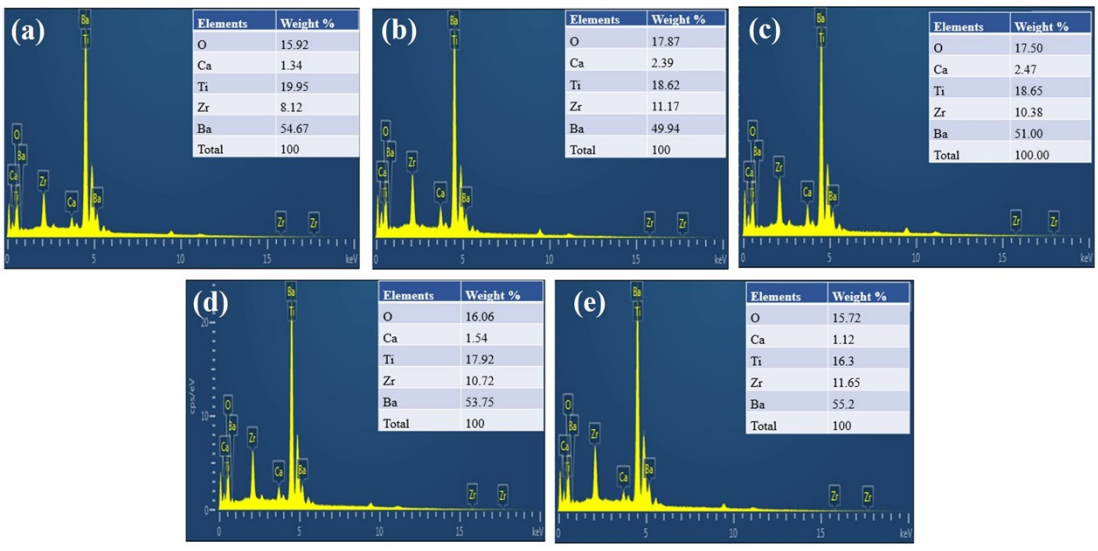

Figure S2 The EDX spectrometer of BZT-*x*BCT (*x*=0.3, 0.4, 0.5, 0.6, 0.7).

Table S1. The weight and atomic percentages of BZT-*x*BCT (*x*=0.3, 0.4, 0.5, 0.6, 0.7) calculated by EDX spectrometer for Ba, Ca, Ti, Zr, O five elements.

	BZT-0.3BCT	BZT-0.4BCT	BZT-0.5BCT	BZT-0.6BCT	BZT-0.7BCT
Element%	Atomic	Atomic	Atomic	Atomic	Atomic
O	52.3	52.1	53.9	54.5	52.0
Ca	1.5	2.0	3.0	2.8	1.7
Ti	**18.1**	19.4	19.2	19.0	**23.0**
Zr	6.8	6.1	5.6	5.8	3.3
Ba	**21.3**	20.4	18.3	17.8	**20.0**

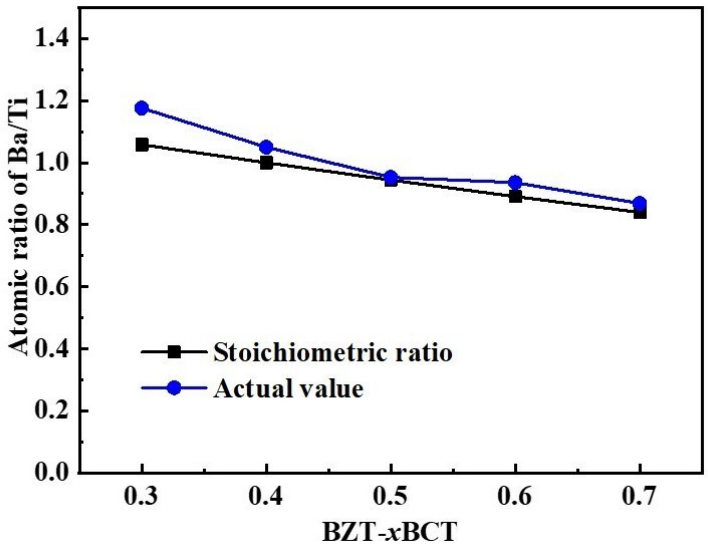

Figure S3. The relative atomic percentage of Ba and Ti in BZT-*x*BCT (*x*=0.3, 0.4, 0.5, 0.6, 0.7) samples.

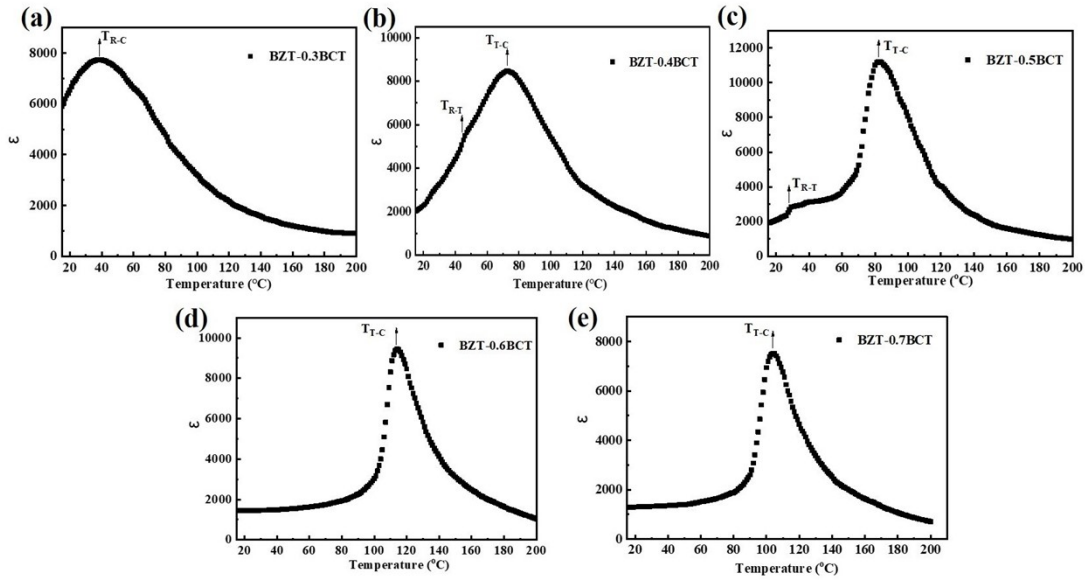

Figure S4. The curve of dielectric permittivity versus temperature for BZT-*x*BCT (*x*=0.3, 0.4, 0.5, 0.6, 0.7) ceramic samples.

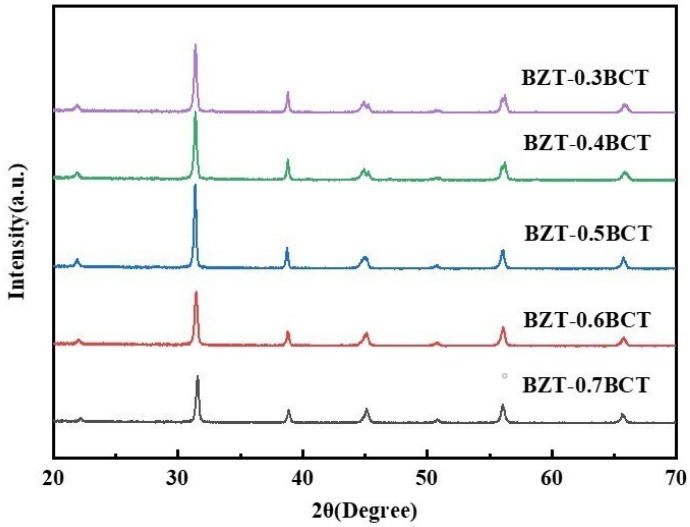

Figure S5. The XRD patterns of BZT-*x*BCT (*x*=0.3, 0.4, 0.5, 0.6, 0.7) ceramic.

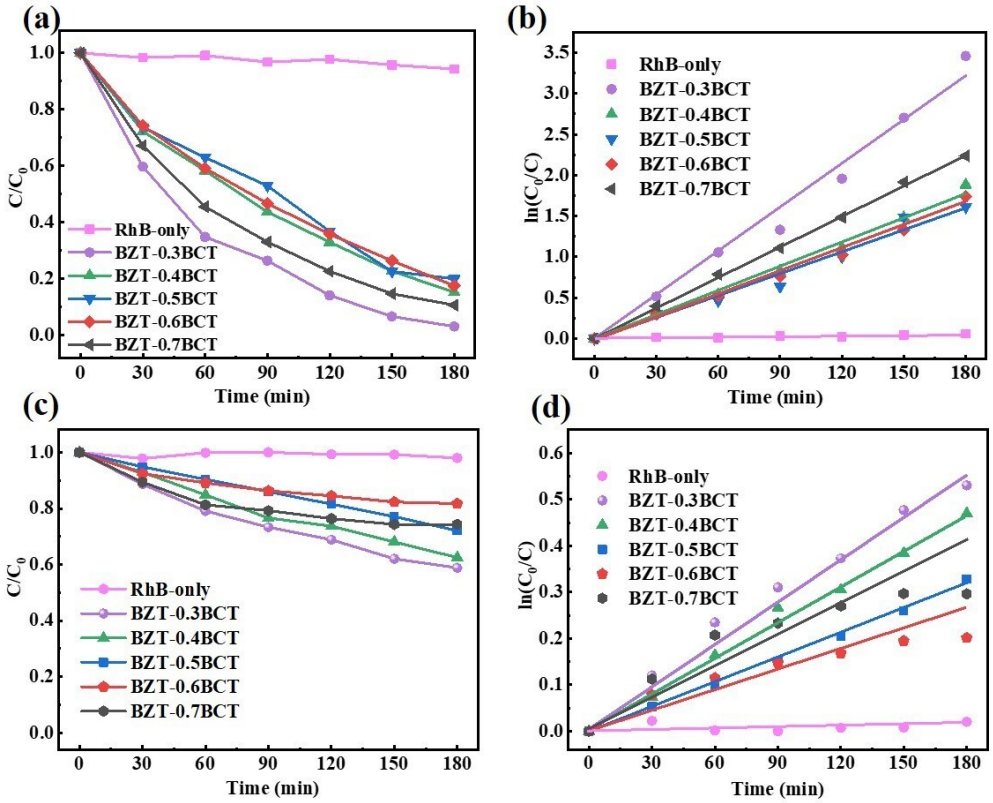

Figure S6. (a, b) The C/C_0 and $\ln(C_0/C)$ of BZT-*x*BCT (*x*=0.3, 0.4, 0.5, 0.6, 0.7) for RhB (5mg/L). (c, d) The C/C_0 and $\ln(C_0/C)$ of BZT-*x*BCT (*x*=0.3, 0.4, 0.5, 0.6, 0.7) for RhB (20mg/L).

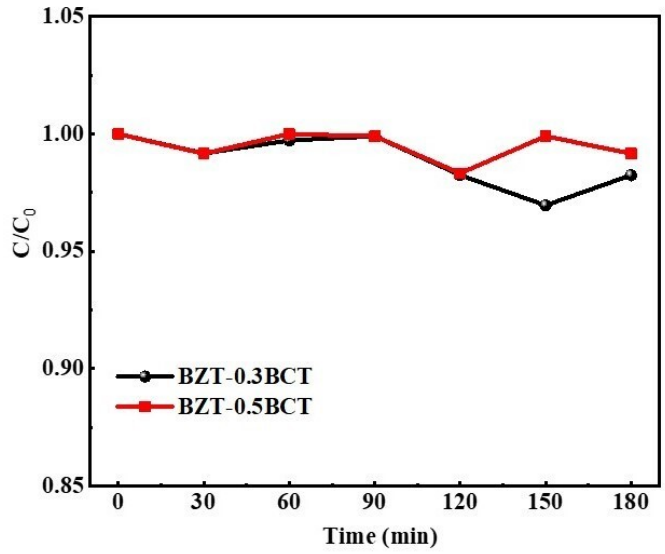

Figure S7. The contribute of pyroelectricity effect to degradation efficiecncy for BZT-0.3BCT and BZT-0.5BCT.

The role of pyroelectricity during the ultrasonication process was also investigated to exclude the effect of changing water to maintain the water temperature stability. The BZT-0.3BCT and BZT-0.5BCT experiment involved the water temperature was carried out by alternated changing between the room temperature and 40°C each 5 min, and low-speed mixing replaced the ultrasonic vibration, the experiment result revealed alternated changed water temperature has negligible influence on the degradation efficiency (Figure. S7).

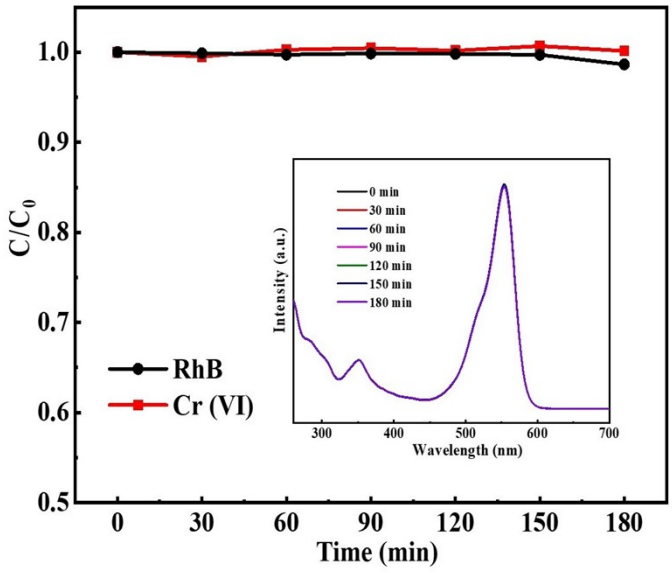

Figure S8. The piezocatalytic performance to degrade RhB and Cr(VI) mixed pollutant without BZT-0.3BCT samples.(The inset shows the UV-Vis absorption spectra of degradation.)

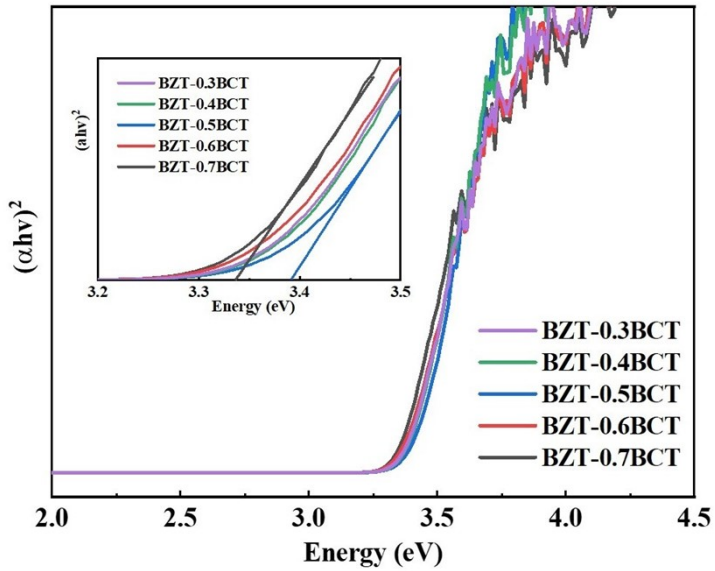

Figure S9. The band gap values of BZT-*x*BCT (*x*=0.3, 0.4, 0.5, 0.6, 0.7) samples.

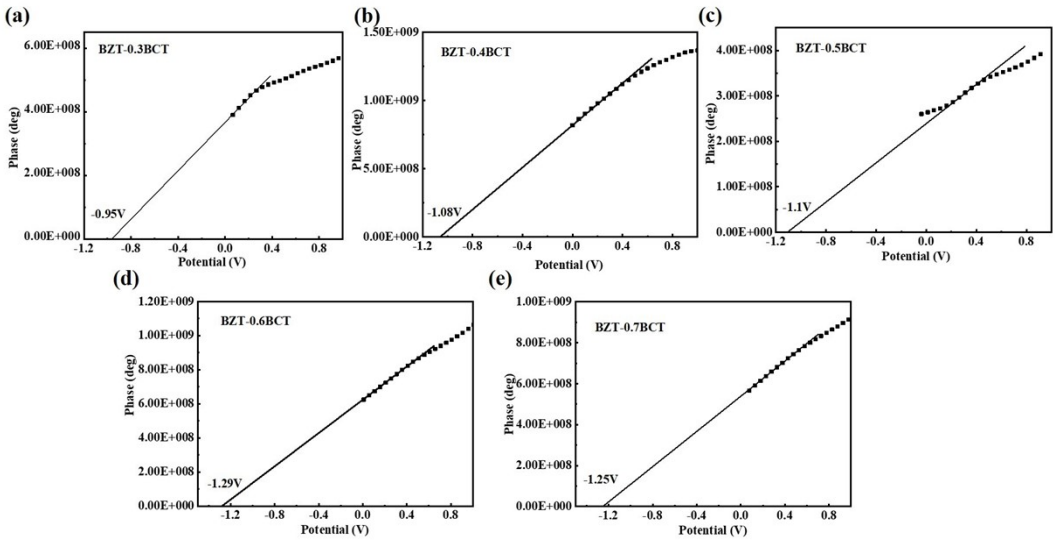

Figure S10. The Mott-Schottky plots of BZT-*x*BCT (*x*=0.3, 0.4, 0.5, 0.6, 0.7) samples.

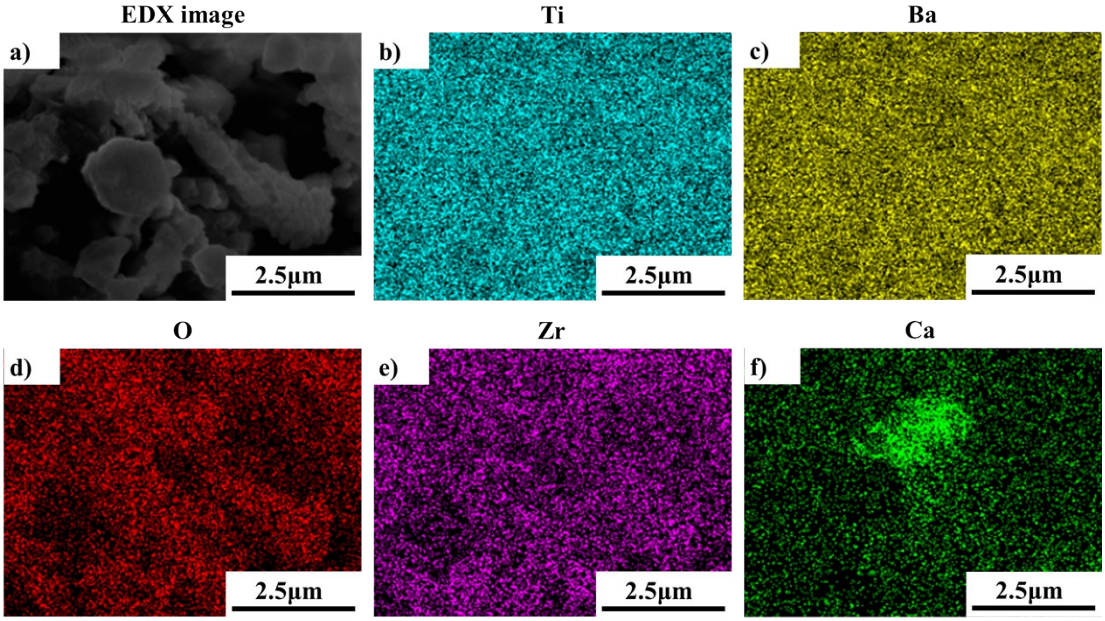

Figure S11. Elemental mapping images of BZT-0.3BCT sample.

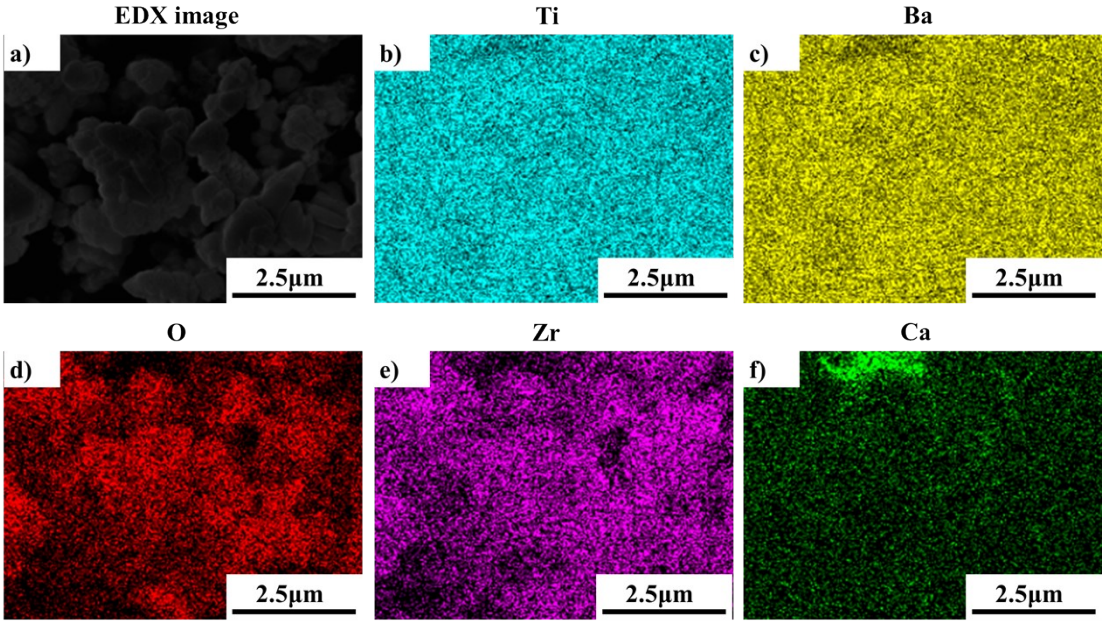

Figure S12. Elemental mapping images of BZT-0.4BCT sample.

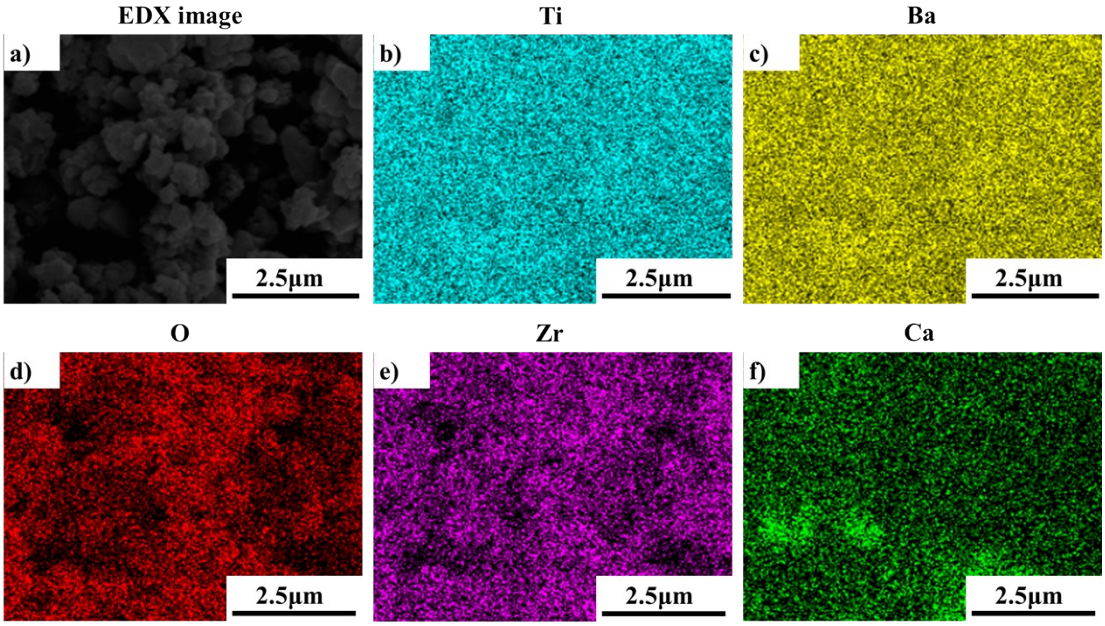

Figure S13. Elemental mapping images of BZT-0.5BCT sample.

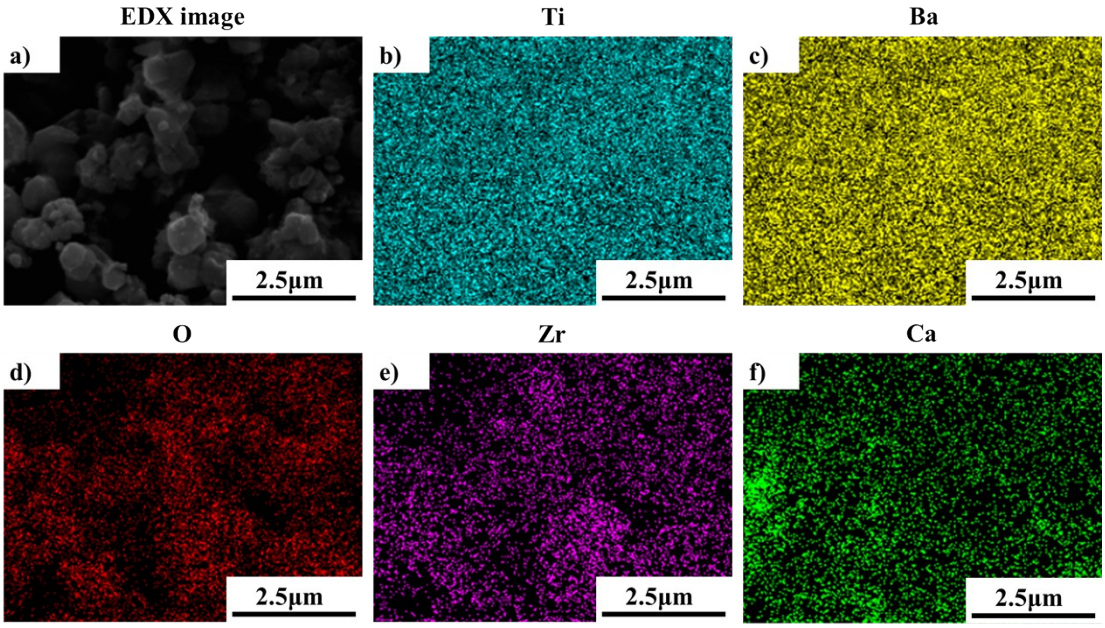

Figure S14. Elemental mapping images of BZT-0.6BCT samples.

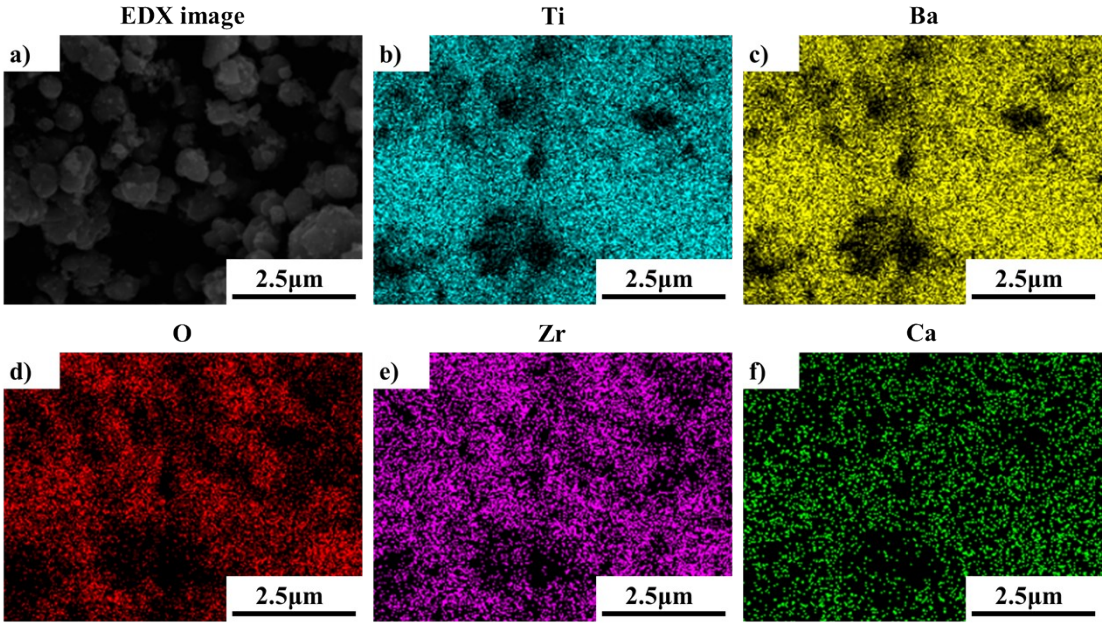

Figure S15. Elemental mapping images of BZT-0.7BCT samples.

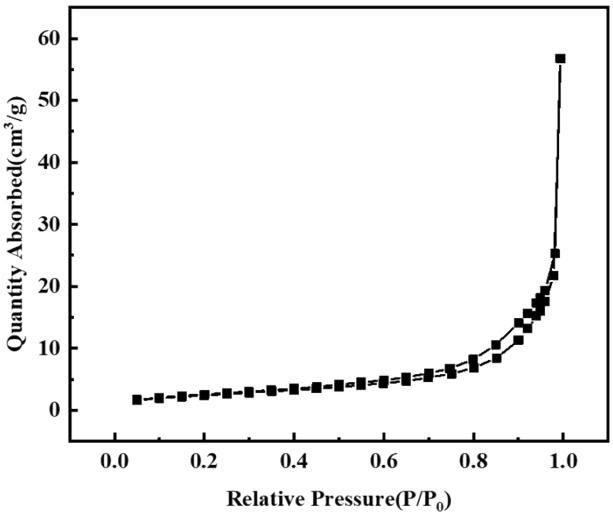

Figure S16. Nitrogen adsorption-desorption isotherms of BZT-0.3BCT nanoparticles.

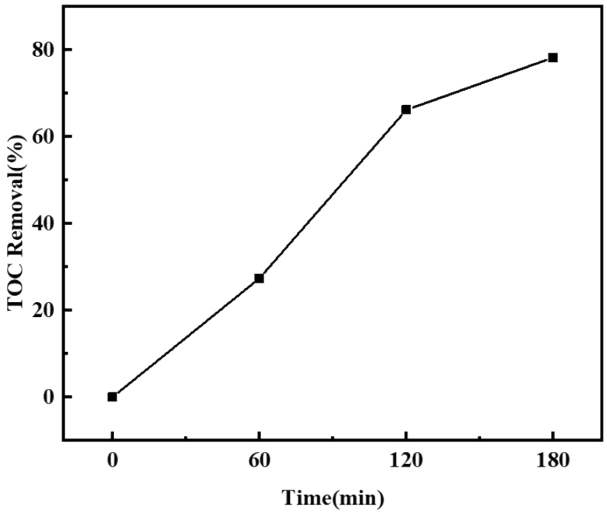

Figure S17. Nitrogen adsorption-desorption isotherms of BZT-0.3BCT nanoparticles.